Crystal Structure of a Pentamidine–Oligonucleotide Complex: Implications for DNA-Binding Properties†

Karen J. Edwards, Terence C. Jenkins, and Stephen Neidle*

Cancer Research Campaign Biomolecular Structure Unit, The Institute of Cancer Research, Sutton, Surrey SM2 5NG, U.K.

Received February 25, 1992

ABSTRACT: The crystal structure of the complex formed between the dodecanucleotide d(CGCGAATTCGCG)$_2$ and the drug pentamidine, which is active against the *Pneumocystis carinii* pathogen in AIDS patients, has been determined to a resolution of 2.1 Å and an *R*-factor of 19.4%. Analysis of the structure has shown the drug to be bound in the 5′-AATT minor groove region of the duplex, with the amidinium groups H-bonded to adenine N3 atoms in an interstrand manner. The drug molecule adopts an extended conformation, and the immediate binding site spans four base pairs. Structural details of the drug–DNA interactions are discussed, and comparison is made with the dodecamer complex of the structurally similar berenil ligand.

Pentamidine [1,5-bis(4-amidinophenoxy)pentane, Figure 1] has established antiprotozoal activity and modest antiviral activity (De Clercq & Dann, 1990), in common with a number of other aromatic diamidines (Bell et al., 1990, and references cited therein). More recently, pentamidine has been found to have activity against the *Pneumocystis carinii* pathogen and has found extensive clinical use in the treatment of *P. carinii* pneumonia, the commonest opportunistic infection in AIDS patients (Sands et al., 1985; Gazzard, 1989; Golden et al., 1989; Wispelwey & Pearson, 1991), which occurs in approximately 80% of these individuals. Several recent studies on pentamidine analogues have been reported (Hughes et al., 1974; Walzer et al., 1988; Jones et al., 1990; Tidwell et al., 1990a,b; Cory et al., 1992) as part of a search for more effective compounds with diminished toxic side effects. Although the mechanism of action against *P. carinii* is unknown at present, there is a correlation between DNA-binding affinity and *P. carinii* activity in a rat model. Thus, the most effective compound in one series of 33 analogues (Tidwell et al., 1990b) is also the strongest DNA-binding agent.

Pentamidine has been shown to bind nonintercalatively to DNA (Zimmer & Wähnert, 1986; Luck et al., 1988), showing a preference for AT-rich DNAs, particularly the synthetic polynucleotide poly(dA)·poly(dT). This behavior is very similar to that exhibited by other nonintercalative AT-selective agents such as netropsin, Hoechst 33258, and berenil, which bind in the minor groove of AT regions in B-form DNA duplexes (Dervan, 1986; Kopka et al., 1985; Coll et al., 1989; Quintana et al., 1991). Footprinting studies reveal that pentamidine binds to AT-rich sequences of DNA (Fox et al., 1990), where the high-affinity binding sites are four to five base pairs (bp) in length. This site size is in accord with a molecular modeling study (Sansom et al., 1990), which suggested that the amidinium groups of the drug could form H-bonded interactions with acceptor atoms of either adenine or thymine bases in the minor groove.

As part of a program of crystallographic studies on the recognition of DNA sequences by synthetic ligands (Brown et al., 1990, 1992), we have cocrystallized pentamidine with the *Eco*RI dodecanucleotide duplex d(CGCGAATTCGCG)$_2$ and determined the structure of the resulting complex.

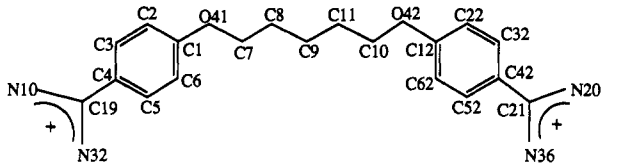

FIGURE 1: Structure of pentamidine.

MATERIALS AND METHODS

Crystallization and Data Collection. The DNA dodecamer d(CGCGAATTCGCG)$_2$ was purchased from Oswel DNA Service (University of Edinburgh, Edinburgh, Scotland, U.K.) and annealed before use. Pentamidine, as the isethionate salt, was obtained from Sigma and used without further purification.

Crystals of the complex were grown by vapor diffusion at 289 K using sitting drops. Long, colorless, needlelike crystals grew from aqueous solutions containing a range of 2-methylpentane-2,4-diol (MPD) precipitant concentrations, with the largest crystals being obtained from droplets containing 5 μL of DNA (10 mg/mL; 3 mM), 5 μL of $MgCl_2$ (100 mM), 4 μL of pentamidine (25 mM; 15 mg/mL) and 5 μL of MPD (50% v/v in 30 mM sodium cacodylate buffer, pH 7.0). The reservoir contained 3 mL of MPD (50% v/v). All solutions were filtered through a 2-μm filter prior to use. Addition of the drug was performed last and resulted in a small amount of precipitation which disappeared after 5–10 min. Crystals grew over a period of 10–14 days. One of size 2.8 × 0.1 × 0.25 mm was mounted in a 0.5-mm quartz capillary with mother liquor and used for data collection. Intensity data were collected at 292 K on a Siemens-Xentronics multiwire area detector using an Enraf-Nonius FR571 rotating anode X-ray generator (40 mA, 65 kV). A crystal-to-detector distance of 8 cm was used, with the 2θ swing angle being fixed to 14°. Two data sets of 500 frames each were obtained at ϕ settings of 0° and 60°, respectively, with a 100° rotation in ω to collect a complete unique data set, using a 0.2° step size. The χ angle was fixed at 45°. Frame scanning, unit cell determination, integration, data reduction and scaling were performed with the XENGEN 1.3 program package. The crystal appeared to have remained stable in the X-ray beam for the duration of the data collection.

Structure amplitudes were based on profile-fitted and simply summed intensities. A total of 10 630 of a possible 14 028 reflections were collected to a resolution of 2.1 Å. These

† This work was supported by the Cancer Research Campaign.
* To whom correspondence should be addressed.

0006-2960/92/0431-7104$03.00/0 Published 1992 by the American Chemical Society

reflections were merged to give 3824 unique reflections (from a possible 4256), with an overall merging R-factor of 6.99%; 2913 of these reflections had intensities greater than the 2σ level. A total of 663 of a possible 685 reflections were observed between 2.2 and 2.4 Å, and 353 of a possible 688 reflections in the range 2.1–2.2 Å.

Structure Solution and Refinement. The unit cell dimensions of the crystal are a = 24.37, b = 40.00, and c = 66.07 Å in the orthorhombic space group $P2_12_12_1$. These cell dimensions are similar to those of the native 12-mer sequence (Dickerson & Drew, 1981) with cell dimensions of a = 24.87, b = 40.39, and c = 66.20 Å, suggesting an isomorphous structure. Accordingly, the coordinates for the native structure deposited in the Brookhaven Data Base (entry no. PDB1BNA) were used as a starting model for the structure solution by molecular replacement. Initial rigid-body constrained–restrained refinement was performed using the program CORELS (Sussman, 1984). The model was initially refined as a duplex against the experimental data, first in the resolution range of 10–4 Å (570 reflections) and subsequently in the range 8–3 Å (1302 reflections). After scaling and five cycles of refinement in each resolution range, the model gave an R-value of 30.7%.

The structure was then divided into 48 rigid groups (comprising 24 nucleosides and 22 phosphate groups, with the O5′ atoms at the 5′-terminus of each strand being defined separately) and refined further against the experimental data to a resolution of 2.5 Å (2227 reflections). After several cycles of CORELS the refinement converged to give an R-factor of 28.7% for the 8–2.5 Å resolution data.

At this stage refinement was continued using the restrained least-squares refinement procedure in the NUCLSQ program (Westhof et al., 1985). All observed data with $[I > 2\sigma(I)]$ between 8 and 2.5 Å was used initially. Successive cycles of refinement reduced the R-factor to 25.0%. Inspection of $2F_o - F_c$ and $F_o - F_c$ electron density maps at this stage showed a good fit for the DNA. A continuous, extended lobe of electron density spanning the four central A·T base pairs in the minor groove was also observed. This lobe of electron density was comparable in size and shape to that of a pentamidine molecule.

Numerous possible water peaks were observed in the difference electron density maps. Only those solvent peaks which were within 2.2–3.4 Å of possible H-bonded partners and which showed good hydration geometries were included in refinement cycles. Solvent peaks were located from $F_o - F_c$ and $2F_o - F_c$ difference electron density maps by using an automated peak search procedure developed by Dr. G. D. Webster in this laboratory.

Although it was possible to fit a model of the pentamidine molecule within the limits of the electron density at this stage, the early image of the ligand was instead ignored while solvent peaks were located in regions outside the minor groove, generally within the major groove or near phosphate oxygens. Positions and temperature factors for the DNA atoms and the oxygen atoms representing water molecules were refined using NUCLSQ. During the next few rounds of refinement the resolution limit was increased to 2.3 Å (2990 reflections), with concurrent adjustment of AFSIG, BFSIG, and scale values. The addition of 33 water molecules at this stage resulted in some improvement in the electron density of the drug and an R-factor of 22.2%.

Coordinates for the pentamidine molecule were obtained from a computer graphics-generated model with an extended $(CH_2)_5$ hydrocarbon chain. This model was manually fitted into the density within the minor groove region of the difference map. Planar groups were assigned to each of the two phenyl rings and the two amidinium moieties of the ligand. The drug was manipulated to fit the curvature of the density using the larger regions at the extremities of the lobe of density to accommodate the phenyl rings. At this stage, little significant density was observed around the amidinium groups.

Refinement of atomic positions and temperature factors for all atoms, including those of the ligand, was continued and the resolution increased to 2.1 Å (3133 reflections); further water molecules were gradually incorporated into the refinement, again adding only those which behaved well.

The position of the drug was monitored with difference "omit" maps at each step of the refinement. These maps were produced by running sets of three refinement cycles, excluding the ligand to remove any bias in F_c values which may be generated by the presence of the drug. After the resolution was increased to 2.1 Å, the drug was refitted manually to cover density which had developed in the amidinium regions of the molecule. The position of the drug was also monitored to check for any bad or close atomic contacts with the DNA.

A total of 79 water molecules were included, to give a final R-factor of 19.4% using 2σ data in the 7–2.1-Å range. Details of the refinement are shown in Table I. Final refined coordinates, together with observed and calculated structure factors, have been deposited in the Brookhaven Data Base (entry no. 1D64).

Table I: Crystallographic and Stereochemical Refinement Parameters for the DNA–Pentamidine Complex

resolution range (Å)	7–2.1	
no. of reflections $[I > 2\sigma(I)]$	3113	
temp (K)	292	
final R;[a] weighted R_w[b] (%)	19.1; 19.8	
distances $>2\sigma$	76	
	rms dev	σ-value
sugar–base bond dist (Å)	0.017	0.025
sugar–base bond angle dist (Å)	0.030	0.040
phosphate bond dist (Å)	0.032	0.030
phosphate angle and H bond dist (Å)	0.041	0.040
planar groups (Å)	0.030	0.030
chiral volumes (Å^3)	0.090	0.100
single torsion contacts (Å)	0.135	0.400
multiple torsion contacts (Å)	0.213	0.400
isotropic temp factors (Å^2)		
sugar–base bonds	5.061	5.00
sugar–base angles	6.078	7.50
phosphate bonds	6.225	7.50
phosphate angles/H bonds	7.618	10.00

[a] $R = \Sigma|F_o - F_c|/\Sigma F_o$. [b] $R_w = ([\Sigma w(F_o - F_c)]^2/[\Sigma(w(F_o)^2]^2])^{0.5}$, where $w = (1/\text{SIGAPP})^2$ and SIGAPP = 2.5 − 30.0(STHOL − 0.166 666 7).

RESULTS

General Features of the Structure. The pentamidine molecule is bound in the AT region of the minor groove of a B-form d(CGCGAATTCGCG)$_2$ double helix (Figure 2). It symmetrically spans over and somewhat beyond the four AT base pairs, with direct H-bonded contacts from the amidinium groups of the drug to N3 of Ade 5 and to N3 of Ade 17 on the opposite strand (Figure 3). These adenines are four base pairs apart. In addition, there are contacts to deoxyribose ring O4′ atoms. There are weaker contacts with the O2 atoms of Cyt 9 and Cyt 21, indicating that the binding-site size requirement for pentamidine extends over slightly more than the four central AT base pairs. There are close contacts from the amidinium groups with the O4′ atoms of Ade 6 and Ade 18, together with a water-mediated contact to O4′ of

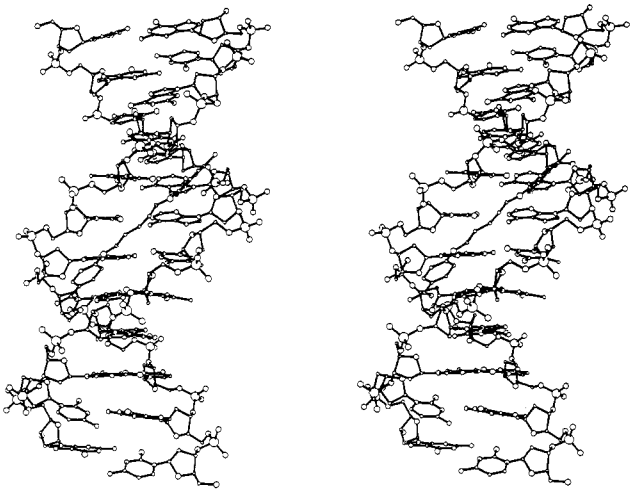

FIGURE 2: Stereoview of the pentamidine–d(CGCGAATTCGCG)$_2$ complex.

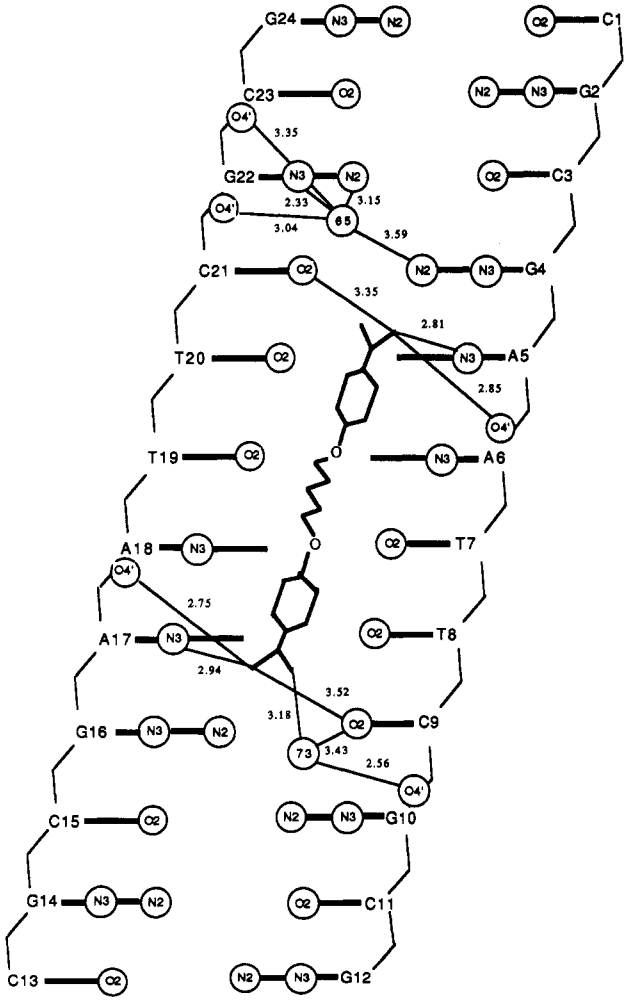

FIGURE 3: Schematic representation of the H-bonded interactions between the amidinium groups of pentamidine and the minor groove of the 12-mer duplex.

Gua 10. In general, these contacts subtend H-bonding angles that deviate far from linearity (Figure 4).

Details of the Groove-Binding Interaction. The two phenyl rings of the bound pentamidine molecule are twisted by 35° with respect to each other (Figure 5), with the effect that the rings are effectively aligned to be parallel to the walls of the minor groove, and thus follow the curvature of the groove walls. Table II gives the torsion angles for the $(CH_2)_5$ linker

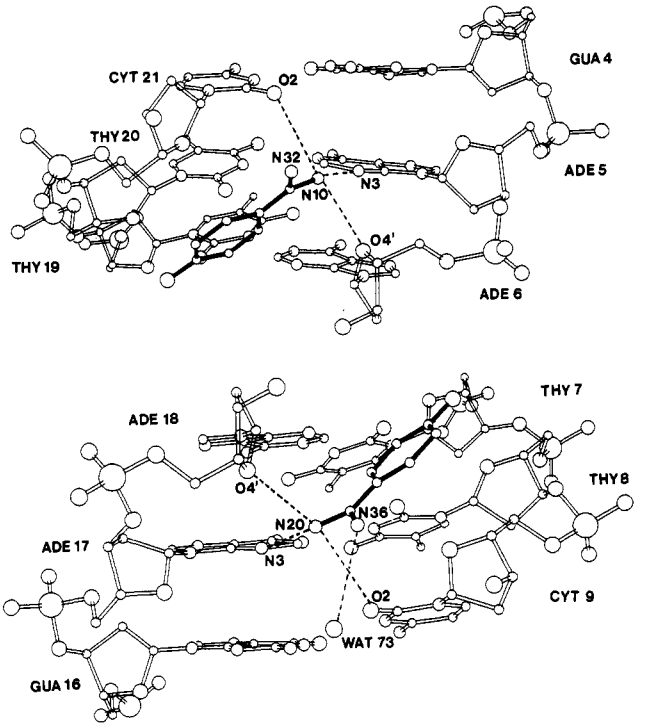

FIGURE 4: Detailed views of the amidinium–DNA interactions showing (A, top) the 5′-end and (B, bottom) the 3′-end of the complex.

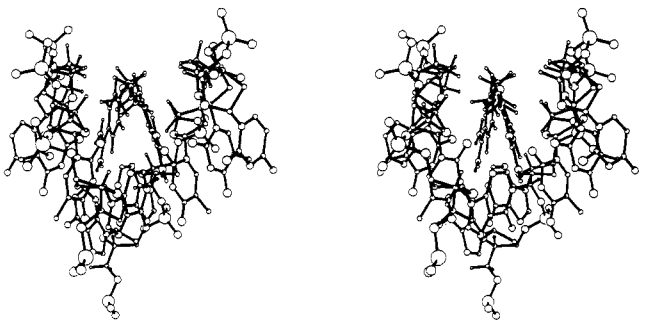

FIGURE 5: Stereoview of the complex, looking along the minor groove of the duplex.

function of the drug. The deviations from 180° pure-staggered values are responsible for the C1···C12 chain length of 9.13 Å, compared to the 9.75 Å distance found in the crystal structure of the free drug molecule (Lowe et al., 1989). This decrease is necessary in order to produce approximate isohelicity with the minor groove. The amidinium groups are twisted out of the planes of the phenyl rings by 3° and −6° at the 5′- and 3′-ends, respectively.

The phenyl rings of the drug contact the floor of the minor grove. We have used the distances between calculated H-atom positions to provide an indication of these contacts. Table III shows that H–C2 of Ade 6 is in close contact with H–C2 on the phenyl ring of the ligand, while H–C3 is in rather weaker contact with H–C2 of Ade 5. The other phenyl ring contacts the opposite strand via H–C2 of Ade 18, through H–C22, and via H–C2 of Ade 17, through H–C32. Thus, the critical nonbonded contacts with the minor groove floor involve

Table II: Torsion Angles for the $O(CH_2)_5O$ Linkage in Pentamidine

torsion	angle (deg)	torsion	angle (deg)
C1–O41–C7–C8	172	C8–C9–C11–C10	−176
O41–C7–C8–C9	−161	C9–C11–C10–O42	175
C7–C8–C9–C11	−156	C11–C10–O42–C12	−179

Table III: Close Atomic Contacts between Pentamidine and DNA[a]

drug	DNA	distance (Å)	drug	DNA	distance (Å)
H–C22	H–C2 (Ade 18)	1.61	H1–C11	H″–C5′ (Thy 20)	1.89
H–C32	H–C2 (Ade 17)	1.95	H2–C11	H–C4′ (Thy 8)	2.14
H–C2	H–C2 (Ade 6)	1.99	C52	H–C4′ (Cyt 9)	2.87
H–C3	H–C2 (Ade 5)	2.34	C62	H–C4′ (Cyt 9)	2.88
H1–C7	H–C4′ (Thy 20)	2.41	C1	H″–C5′ (Cyt 21)	2.70
H2–C7	H–C2 (Ade 6)	2.39	C6	H–C4′ (Cyt 21)	2.50
H1–C8	H–C4′ (Thy 20)	1.93	C6	H″–C5′ (Cyt 21)	2.52
H2–C8	H″–C5′ (Thy 8)	2.43	C5	H–C4′ (Cyt 21)	2.14
H2–C10	H–C2 (Ade 18)	2.55			

[a] Estimated standard deviation for distances is ±0.3 Å.

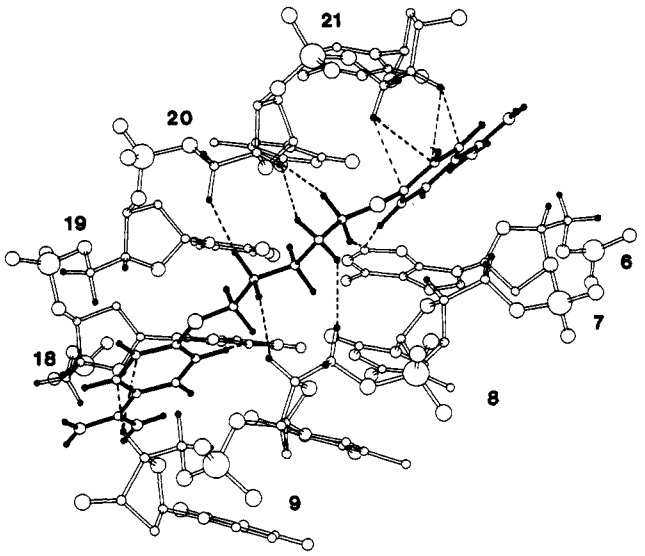

FIGURE 6: View of the interactions between backbone H4′ and H5′ atoms within the binding site and atoms of the drug molecule. The bonds of the drug molecule are shaded. All H atoms are in calculated positions.

three adenines of the base pairs at and close to the center of the binding site (Figure 5), with a fourth adenine (Ade 5) having a lesser involvement. Weak contacts are also achieved between H–C2 of Ade 5 and the central carbon atom C19 of the 5′-end amidinium group of the ligand, and between H–C2 of Ade 17 and the corresponding C21 atom at the 3′-end, at separations of 3.27 and 3.25 Å, respectively. The H–C2 atoms of Ade 6 and Ade 18 are also in contact with one H atom from each end of the $(CH_2)_5$ hydrocarbon chain. The majority of the hydrogen atoms within this chain are themselves in close contact with the H atoms attached to the C4′ and C5′ sugar atoms on the DNA backbone (Figures 5 and 6 and Table III). Such contacts are at the mouth of the groove (Neidle, 1992) and may be major factors in the stabilization of the complex, together with favorable contacts from H4′ and H5′ sugar protons with the phenyl rings of the drug. Figure 7 shows that the minor groove is mostly unchanged in width compared to that in other isomorphous minor groove complexes with, for example, berenil (Brown et al., 1990). A detailed comparison with the berenil–d(CGCGAATTCGCG)$_2$ complex shows some differences. There is an increase of ~1 Å in the P···P width at one point (Cyt 11···Ade 18) compared to the berenil complex. There are also increases in several of the interstrand H4′···H5′ and H5′···H4′ separations (Figure 7). These latter increases are mostly in the central region of the duplex and probably reflect the increased van der Waals size of the linker chain in pentamidine (seven atoms) compared to the linear triazene (three atoms) linkage of berenil. The higher mobility of the hydrocarbon chain, as evidenced by its

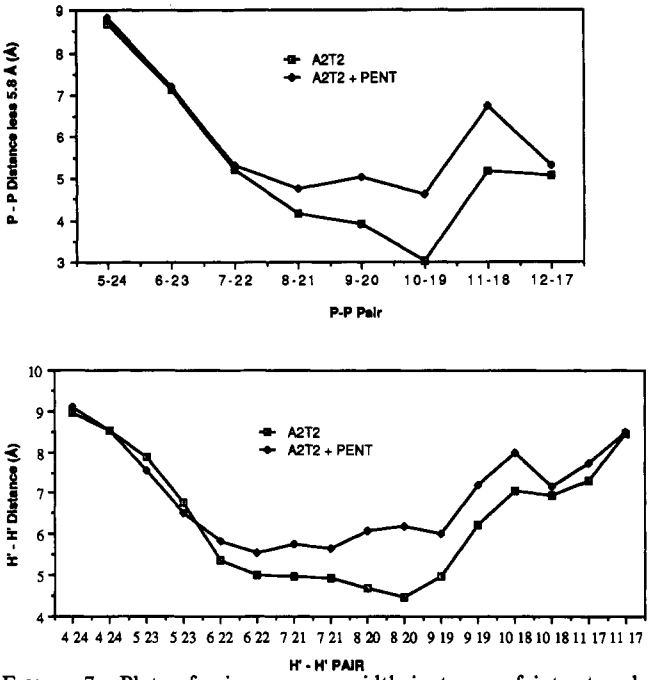

FIGURE 7: Plots of minor groove width in terms of interstrand separation for the native dodecamer and the complex with pentamidine: (A, top) Interstrand P···P distances. (B, bottom) Interstrand H4′···H5′ and H5′···H4′ distances between atoms of a residue on one strand and the (n+3)th residue on the second strand.

temperature factors, may also play a role in the groove opening observed for pentamidine.

The binding of pentamidine in the minor groove effectively displaces the "spine of hydration" determined for the native 12-mer (Drew & Dickerson, 1981). However, one of the water molecules found in the present study, WAT65, corresponds almost exactly in terms of contacts to the first water molecule in this spine, at the 5′-end of the helix. This water molecule bridges between N2 and N3 of Gua 22 (Figure 3) as well as to successive O4′ atoms on this strand. A second water molecule, WAT73, corresponds to a position midway between the second-last and the last waters at the 3′-end of the spine. By contrast to WAT65, this water molecule is in H-bonded contact with an amidinium group of the drug, bridging it to the O4′ atom of Cyt 9. There is also a network of water molecules extending over the mouth of the minor groove, with a weak interaction (3.41 Å distant) between the O42 ether oxygen atom of the ligand and one of these water molecules (WAT80), which then interacts with a phosphate oxygen atom of Thy 19 (3.04 Å).

Conformational Features. The binding of pentamidine to the dodecamer produces very few significant changes in helical or base-pair geometry compared to either the native 12-mer or its complexes with other minor groove drugs, including netropsin (Kopka et al., 1985), Hoechst 33258 (Pjura et al., 1987), and berenil (Brown et al., 1990). Values for the base-pair and base-step morphological parameters are given in Table IV.

DISCUSSION

This study has established that pentamidine acts as a "classic" DNA minor groove-binding drug. In common with berenil, where bis(phenylamidinium) groups are also present, the strongly cationic ends of the drug are positioned deep in the groove rather than close to phosphate groups. The pentamidine ligand occupies a binding site that spans four to five base pairs, in accord with footprinting (Fox et al., 1990) and

Table IV: Helical Parameters for the Dodecamer

base-pair parameters					base-pair step parameters				
base pair	propeller twist (deg)	buckle (deg)	tip (deg)	inclin (deg)	base step	twist (deg)	roll (deg)	tilt (deg)	slide (Å)
C1·G24	−15	−12	0	8	C1pG2	36	6	0	0.4
G2·C23	−10	4	1	9	G2pC3	40	− 5	3	0.7
C3·G22	− 3	0	−10	8	C3pG4	32	6	4	0.9
G4·C21	−12	− 7	− 8	7	G4pA5	34	8	0	−0.1
A5·T20	−16	− 7	− 3	3	A5pA6	37	2	−1	−0.5
A6·T19	−18	0	− 1	0	A6pT7	30	− 3	2	−0.5
T7·A18	−18	− 2	− 5	1	T7pT8	38	5	1	0.0
T8·A17	−20	− 1	0	0	T8pC9	36	0	0	0.1
C9·G16	−10	10	0	1	C9pG10	33	0	−3	1.1
G10·C15	− 1	−12	1	− 2	G10pC11	40	−11	0	0.9
C11·G14	−30	− 2	− 8	− 4	C11pG12	39	− 8	0	0.6
G12·C13	−20	−10	−11	−20					

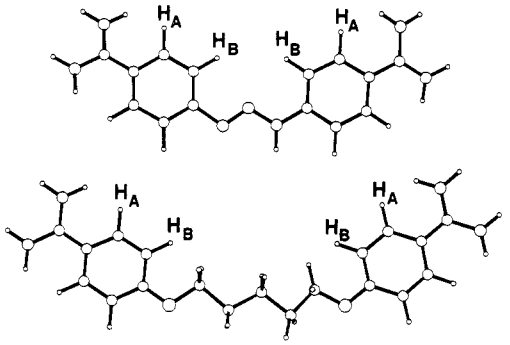

FIGURE 8: Comparison of the berenil (top) and pentamidine (bottom) ligand molecules, showing the conformations as determined in their d(CGCGAATTCGCG)$_2$ complexes. H atoms are shown in their calculated positions.

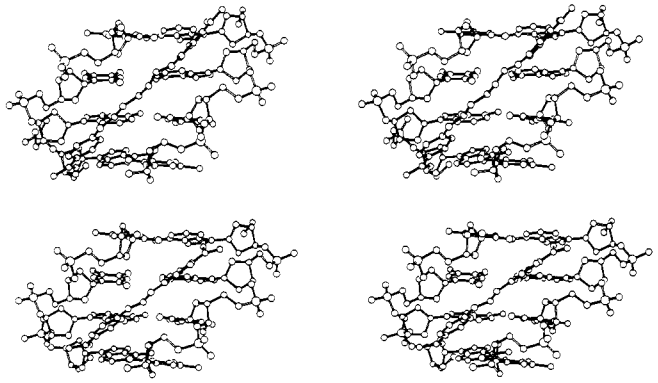

FIGURE 9: Comparative stereoviews of the complexes formed with the 12-mer by pentamidine (top) and berenil (bottom) molecules. Nucleotides 5–8 (first strand) and 17–20 (second strand) are shown.

other biophysical data. We observe that the interaction involves a pair of adenine bases which are separated by two spanned base pairs, in a 1,4-interstrand manner. Berenil has been found to interact with 1,3-interstrand adenines in both its crystal and solution complexes with this sequence (Brown et al., 1990; Lane et al., 1991) and to 1,4-interstrand thymines in its complex with d(CGCAAATTTGCG)$_2$ (Brown et al., 1992). This last structure is probably a special case, with the 5′-AAATTT sequence having distinct effects on several base-pair parameters that result in altered positions for the base-pair edges in the minor groove.

The pentamidine ligand, in common with berenil and other minor groove-binding drugs, is in close contact with the H atoms attached to the adenine C2 atoms that are on the floor of the minor groove. These close contacts are with Ade 6, Ade 17, and Ade 18 (and to a lesser extent with Ade 5) and involve the four inner-face H atoms on the two phenyl residues of the drug (Figures 8 and 9). Substitution of these adenines by guanines, with sterically bulky exocyclic amino groups at the 2-position, would thus be very disfavored. Berenil, in its crystal complex with d(CGCGAATTCGCG)$_2$ (Brown et al., 1990), makes close contacts solely with Ade 6 and Ade 18, with involvement of only one H atom on each phenyl ring (H_A in Figure 8). Thus, the observed AT sequence preference for binding shown by both drugs (Portugal & Waring, 1987; Fox et al., 1990; Laughton et al., 1990) is, at least in structural terms, a combination of positive and negative effects: the H-bonding to adenines from the amidinium moieties of the drug, the narrowed minor groove in the AT-rich tract, and steric hindrance due to guanines within the central two base pairs of the binding site. The sequence 5′-AATT is among the more strongly preferred DNA sequences for pentamidine binding as shown by footprinting for the *tyr*T fragment (Fox et al., 1990). However, the preferences revealed for d(·TTTT·) and d(·AAAA·) sequences by this method suggest that pentamidine may also form interstrand H bonds between an adenine and a thymine base, with perhaps a preference for the particular structural features shown by oligo(dA) tracts. The minimum AT site size for pentamidine is three to four base pairs, on the basis of contacts that we see on the minor groove floor. This size is entirely in accord with that determined by hydroxyl radical footprinting (Fox et al., 1990). Similarly, the minimum berenil AT site size requirement is two base pairs, again in accord with hydroxyl radical footprinting studies (Laughton et al., 1990). The fact that, for both berenil and pentamidine, the size of the AT region of the binding site is less than the total binding site size is indicative of a tolerance for GC base pairs, as is indeed found experimentally.

It is at first sight surprising that pentamidine binding to 5′-AATT only requires one more base pair than berenil, even though it has four more atoms linking the two phenyl rings. The intermolecular separation between the pair of H_A atoms for pentamidine in the complex (Figure 8) is 10.7 Å, and 7.1 Å in berenil. The corresponding $H_B \cdots H_B$ separations for pentamidine and berenil are 6.8 and 2.9 Å, respectively. Both drugs have their critical contacts with the minor groove floor to Ade 6 and Ade 18 (Table III). This may be a major factor in their positioning along the groove (Figure 5). The H-bonding from the amidinium groups of berenil extends both up and down the groove, outward from the drug molecule to adenine N3 atoms. Even so, a water molecule is required as a bridge in order for it to contact Ade 5, whereas Ade 18 is H-bonded directly to the other end of a bound berenil molecule. In contrast, the pentamidine molecule covers more than four base pairs (Figure 9). Its amidinium groups are oriented rather more toward base pairs A5·T20 and T8·A17 than to the outer ones, thus ensuring a 4-bp site. Presumably the contacts with the H–C2 atoms of Ade 6 and Ade 18 play a role in maintaining

this position rather than one translated along the groove by 1–1.7 Å, which could result in a 1,5-binding model.

Implications for the DNA Binding of Pentamidine Analogues. We have examined a number of pentamidine derivatives for possible modes of interaction with the d(CGCGAATTCGCG)$_2$ duplex, using the present structure as a starting point. Calculations of intermolecular energetics will be reported elsewhere; we describe here some qualitative observations of the effects of changes to the pentamidine motif in the light of published DNA-binding data. Such an approach may lead to the rational design of new analogues with superior DNA-binding properties. These may, in turn, relate to improved inhibition of *P. carinii* (Tidwell et al., 1990a,b; Cory et al., 1992).

(i) Replacement of the $(CH_2)_5$ chain by $(CH_2)_3$ would result in a 3- rather than 4-bp binding site, with the potential for at least one of the amidinium groups to bridge between adjacent adenines, with H-bonded interactions to both. This suggests an increased DNA-binding affinity compared to pentamidine; a 40% increase in the thermal denaturation temperature (T_m) for the DNA–drug complex is reported (Cory et al., 1992).

(ii) Introduction of relatively hydrophobic methoxy substituents at positions meta to the amidinium moieties of each phenyl ring of the drug would result in close (2.1–2.3 Å) contacts between the methoxy H atoms and sugar H4′, H5′ atoms of the DNA backbone. These are stabilizing effects and are confirmed experimentally by a ~15% increase in T_m-value for both pentamidine and its $(CH_2)_3$ homologue.

ACKNOWLEDGMENT

Drs. Jane Skelly and David Brown of this laboratory are thanked for much practical help. We are indebted to Dr. Michael Cory (Burroughs Wellcome Co.) for discussion and provision of unpublished data.

REFERENCES

Bell, C. A., Hall, J. E., Kyle, D. E., Grogl, M., Ohemeng, K. A., Allen, M. A., & Tidwell, R. R. (1990) *Antimicrob. Agents Chemother. 34*, 1381–1386.

Brown, D. G., Sanderson, M. R., Skelly, J. V., Jenkins, T. C., Brown, T., Garman, E., Stuart, D. I., & Neidle, S. (1990) *EMBO J. 9*, 1329–1334.

Brown, D. G., Sanderson, M. R., Garman, E., & Neidle, S. (1992) *J. Mol. Biol.* (in press).

Coll, M., Aymami, J., van der Marel, G., van Boom, J. H., Rich, A., & Wang, A. H.-J. (1989) *Biochemistry 28*, 310–320.

Cory, M., Tidwell, R. R., & Fairley, T. A. (1992) *J. Med. Chem. 35*, 431–438.

De Clercq, E., & Dann, O. (1990) *J. Med. Chem. 23*, 787–795.

Dervan, P. B. (1986) *Science 232*, 464–471.

Dickerson, R. E., & Drew, H. R. (1981) *J. Mol. Biol. 149*, 761–786.

Drew, H. R., & Dickerson, R. E. (1981) *J. Mol. Biol. 151*, 535–556.

Fox, K. R., Sansom, C. E., & Stevens, M. F. G. (1990) *FEBS Lett. 266*, 150–154.

Gazzard, B. G. (1989) *J. Antimicrob. Chemother. 23*, 67–75.

Golden, J. A., Chernoff, D., Hollander, H., Feigal, D., & Conte, J. E. (1989) *Lancet* 654–657.

Hughes, W. T., McNabb, P. C., Makres, T. D., & Feldman, S. (1974) *Antimicrob. Agents Chemother. 5*, 289–293.

Jones, S. K., Hall, J. E., Allen, M. A., Morrison, S. D., Ohemeng, K. A., Reddy, V. V., Geratz, J. D., & Tidwell, R. R. (1990) *Antimicrob. Agents Chemother. 34*, 1026–1030.

Kopka, M. L., Yoon, C., Goodsell, D., Pjura, P., & Dickerson, R. E. (1985) *J. Mol. Biol. 183*, 553–563.

Lane, A. N., Jenkins, T. C., Brown, T., & Neidle, S. (1991) *Biochemistry 30*, 1372–1385.

Laughton, C. A., Jenkins, T. C., Fox, K. R., & Neidle, S. (1990) *Nucleic Acids Res. 18*, 4479–4488.

Lowe, P. R., Sansom, C. E., Schwalbe, C. H., & Stevens, M. F. G. (1989) *J. Chem. Soc., Chem. Commun.* 1164–1165.

Luck, G., Zimmer, C. H., & Schweizer, D. (1988) *Stud. Biophys. 125*, 107–119.

Neidle, S. (1992) *FEBS Lett. 298*, 97–99.

Portugal, J., & Waring, M. J. (1987) *Eur. J. Biochem. 167*, 281–289.

Pjura, P. E., Grzeskowiak, K., & Dickerson, R. E. (1987) *J. Mol. Biol. 197*, 257–271.

Quintana, J. R., Lipanov, A. A., & Dickerson, R. E. (1991) *Biochemistry 30*, 10294–10306.

Sands, M., Kron, M. A., & Brown, R. B. (1985) *Rev. Infect. Dis. 7*, 625–634.

Sansom, C. E., Laughton, C. A., Neidle, S., Schwalbe, C. H., & Stevens, M. F. G. (1990) *Anti-Cancer Drug Des. 5*, 243–248.

Sussman, J. L. (1984) in *Methods and Applications in Crystallographic Computing* (Hall, S. R. & Ashida, T., Eds.) pp 206–237, Clarendon Press, Oxford, U.K.

Tidwell, R. R., Jones, S. K., Geratz, J. D., Ohemeng, K. A., Bell, C. A., Berger, B. J., & Hall, J. E. (1990a) *Ann. N. Y. Acad. Sci. 616*, 421–441.

Tidwell, R. R., Jones, S. K. Geratz, J. D., Ohemeng, K. A., Cory, M., & Hall, J. E. (1990b) *J. Med. Chem. 33*, 1252–1257.

Walzer, P. D., Kim, C. K., Foy, J., Linke, M. J., & Cushion, M. (1988) *Antimicrob. Agents Chemother. 32*, 896–905.

Westhof, E., Dumas, P., & Moras, D. (1985) *J. Mol. Biol. 184*, 119–145.

Wispelwey, B., & Pearson, R. D. (1991) *Infect. Control Hosp. Epidemiol. 12*, 375–382.

Zimmer, C., & Wähnert, U. (1986) *Prog. Biophys. Mol. Biol. 47*, 31–112.